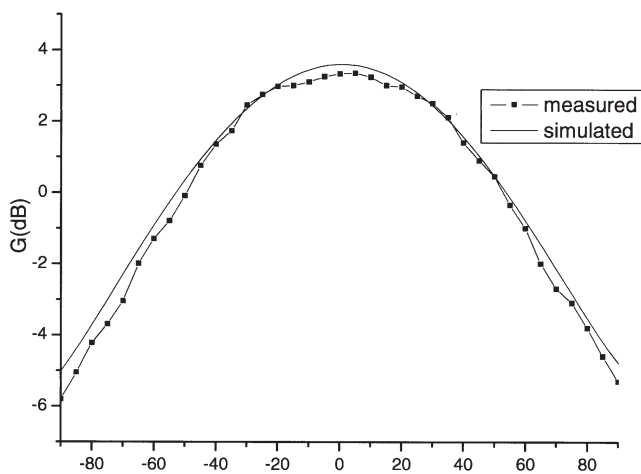


(a)



(b)

Figure 6 Measured and simulated radiation patterns (a) x - z plane; (b) y - z plane

3. EXPERIMENTAL RESULTS

A test antenna was fabricated and measured based on the simulated results, and a photograph of the antenna is shown in Figure 3, with dimensions $a = 61$ mm, $h_1 = 5$ mm, $\epsilon_{r1} = 3.0$, $W_{a1} = W_{a2} = 1.5$ mm, $L_{a1} = 30$ mm, $L_{a2} = 12$ mm, $W_{a1} = W_{a2} = 2$ mm, $L_{b1} = 11$ mm, $L_{b2} = 20$ mm, $h = 0.5$ mm, $\epsilon_r = 2.55$, and $L_s = 9.25$. Figure 4 gives the measured return loss, where its measured impedance bandwidth for $S_{11} \leq -10$ dB covers 879.6–1403.75 MHz (45.9%). Figure 5 shows the measured axial ratio and the gain of antenna. The measured axial ratio is better than 2 dB at 1137–1348 MHz, i.e., 2 dB circularly polarized (CP) bandwidth is 17% with the center frequency of 1242.5 MHz. The antenna gain is better than 1 dB at 1163–1298 MHz (11%). Figure 6 shows the antenna radiation patterns in x - z plane and y - z plane, where the simulated results agree well with the measured ones, verifying the validity of the simulation.

4. CONCLUSION

A new design of broadband circularly polarized antenna has been presented with its simulated and experimental results. It has been measured that its 10 dB return-loss bandwidth is 45.9% (879.6–1403.75 MHz), and the 2 dB axial-ratio CP bandwidth is 17% (1137–1348 MHz), while 1 dB gain bandwidth is 11% (1163–1298 MHz). Since the antenna is of low profile, compact structure and easy fabrication, it is attractive for the ground terminal receiver of satellite communication system and other wideband circularly polarized applications. To decrease the back radiation and enhance the gain, a reflective ground may be added at the rear of the antenna.

REFERENCES

1. D.M. Pozar and S.M. Duffy, A dual-band circularly polarized aperture-coupled stacked microstrip antenna for global positioning satellite, *IEEE Trans Antenn Propag* 45 (1997), 1618–1625.
2. H.M. Chen, Y.F. Lin, and T.W. Chiou, Broadband circularly polarized aperture-coupled microstrip antenna mounted in a 2.45 GHz wireless communication system, *Microwave Opt Technol Lett* 28 (2001), 100–102.
3. H. Kim, B.M. Lee, and Y.J. Yoon, A single-feeding circularly polarized microstrip antenna with the effect of hybrid feeding, *IEEE Antenn Wireless Propag Lett* 51 (2003), 74–77.
4. X.M. Qing, Broadband aperture-coupled circularly polarized microstrip antenna fed by a three-stub hybrid coupler, *Microwave Opt Technol Lett* 40 (2004), 38–41.
5. K.L. Lau and K.M. Luk, A novel wide-band circularly polarized patch antenna based on L-probe and aperture-coupling techniques, *IEEE Trans Antenn Propag* 53 (2005), 577–580.
6. K.L. Lau and K.M. Luk, A wide-band circularly polarized L-probe coupled patch antenna for dual-band operation. *IEEE Trans Antenn Propag* 53 (2005), 2636–2644.

© 2006 Wiley Periodicals, Inc.

DESIGN AND DOUBLE NEGATIVE PROPERTY VERIFICATION OF C BAND LEFT-HANDED METAMATERIAL

Fan-Yi Meng,¹ Qun Wu,¹ Bo-Shi Jin,¹ Hai-Long Wang,¹ and Jian Wu²

¹ School of Electronics and Information Technology
Harbin Institute of Technology
Harbin, Heilongjiang, 150001 People's Republic of China
² National Key Laboratory of Electromagnetic Environment
Beijing 102206 People's Republic of China

Received 11 February 2006

ABSTRACT: In this article, a left-handed (LH) metamaterial with miniaturized unit cell and broad bandwidth is designed. Its relative bandwidth is 56.4%, and the unit cell electrical size is 0.067 at the central frequency where the LH metamaterial is available. The effective permittivity and effective permeability are extracted from the transmission and reflection data at normal incidence for the LH metamaterial proposed here. The double negative (DNG) property is shown by the simultaneously negative effective permittivity and effective permeability and is confirmed by the equivalent circuit. © 2006 Wiley Periodicals, Inc. *Microwave Opt Technol Lett* 48: 1732–1736, 2006; Published online in Wiley InterScience (www.interscience.wiley.com). DOI 10.1002/mop.21763

Key words: left-handed metamaterial; miniaturized unit cell; broad bandwidth; double negative property

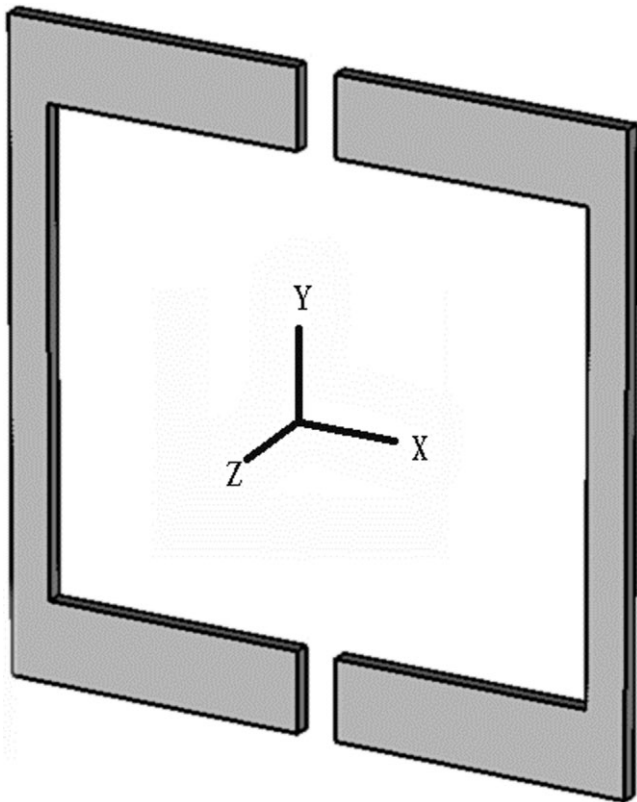


Figure 1 Unit cell of LH metamaterial

1. INTRODUCTION

In recent years, left-handed (LH) metamaterial with simultaneously negative permittivity and permeability have attracted a great deal of attention in the fields of solid-state physics, materials science, optics, and applied electromagnetics [1]. In 1968, the Russian physics scientist Veselago proposed the basic theories about LH metamaterial characteristics, and pointed out that many electromagnetic properties of LH metamaterial are opposite compared with that of conventional material, including Doppler effect, Cherenkov effect, and Snell's law [2]. However, the research about LH metamaterial was slowly developed in about 30 years after Veselago's pioneering work, because the LH metamaterial has not been found in nature until now. In 1998, Pendry et al. pointed out that the negative permittivity effect could be exhibited by a periodic wire array [3]. In 1999, the negative permeability effect of the periodic split ring resonators (SRRs) array was also presented by Pendry et al. [4]. On the basis of these results, in 2000, Smith first fabricated LH metamaterial by reasonably arranging the array with rods and SRRs [5]. However, the performance of the initial LH metamaterial was not so good that it could not be used for application due to the drawback of high loss, narrow band, and large dimension. From this point, many types of LH metamaterial such as the ones consisting of a periodic arrangement of the capacitively loaded strips and the SRRs [6], the deformed rods and SRRs structure [7], the double S-shaped resonators [8], and also transmission line [9] are designed and fabricated to broaden the bandwidth and to lower the loss of LH metamaterial, recently. However, broad bandwidth and low loss alone are not sufficient for the application of LH metamaterial; what's more, the miniaturized structural unit cell is needed, because

the parasitic diffraction effects are necessarily present with increasing importance when the unit cell electrical size, which is defined as ratio of unit cell size in the propagation direction of the electromagnetic wave to the operating wavelength, approaches 0.25. These effects include poor refraction, characterized by diffuse focal spots comparable to those caused by optical aberrations, diffraction losses due to the scattering occurring at each cell, and restriction of the operation bandwidth.

In view of this consideration, a C band planar LH metamaterial, whose unit electrical cell size is 0.067 and relative bandwidth is 56.4%, is designed with CST's microwave studio (MWS) simulation tools. The reflection (S_{11}) and transmission (S_{21}) results are given for the scattering of the normally incident plane wave from the double negative (DNG) metamaterial slab constructed from the split square ring resonator (SSRR). The effective permittivity and effective permeability of the LH metamaterial are extracted from the reflection and transmission data based on Nicolson–Ross–Weir (NRW) approach [6]. The calculated results show that the effective permittivity and effective permeability are simultaneously negative within 4.2~7.5 GHz. In addition, in order to verify the DNG property, the reflection (S'_{11}) and transmission (S'_{21}) for the scattering of the normally incident plane wave from an ideal uniform LH metamaterial slab described by the Drude model, which is equivalent to the composite one, are numerically simulated. Results show that S'_{11} and S'_{21} are in good agreement with S_{11} and S_{21} for both magnitude and phase, respectively.

2. DESIGN OF MINIATURIZED PLANAR LH METAMATERIAL

According to transmission line theory, LH metamaterial can exist as long as there are the distributed shunt inductance and series capacitance simultaneously; and the performance of LH metamaterial will be good, if the frequency response of the shunt inductance and series capacitance is stable [9]. From this point, a LH metamaterial unit cell consisting of SSRRs and embedded medium is designed, as shown in Figure 1. It is expected that the gaps in X direction can produce a strong series capacitor-like response and the strips in Y direction can produce a strong shunt inductor-like response, when the unit cell is illuminated by normally incident plane wave with parallel polarization. In this case, the equivalent circuit of SSRR can be drawn, as shown in Figure 2. The C_1 and L_1 are the series capacitance and shunt inductance, which can be, respectively, expressed as

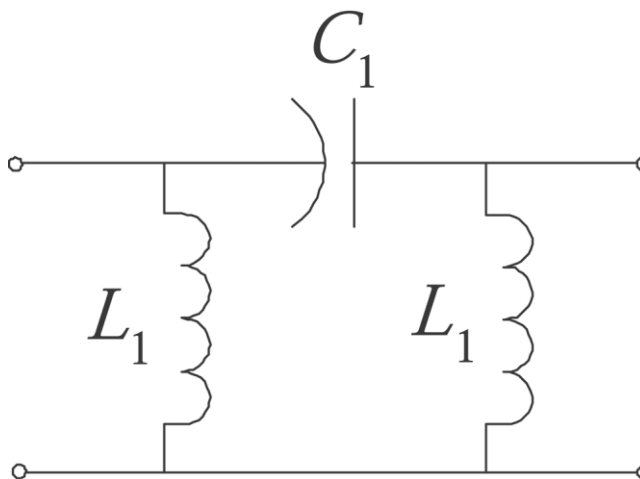


Figure 2 Equivalent circuit of the unit cell

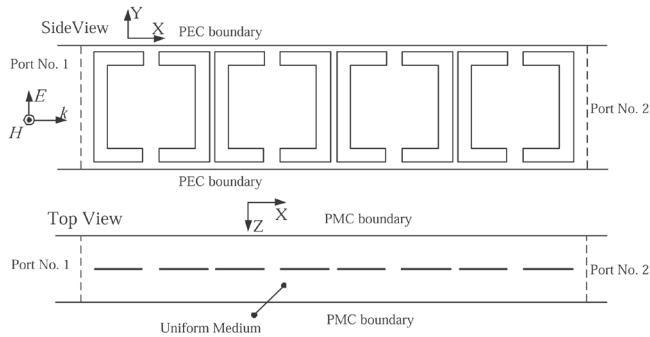


Figure 3 Simulation model of the LH metamaterial slab

$$L_1 = \mu_0 \frac{\ln(d/r)}{4\pi}, \quad (1)$$

$$C_1 = 2.2 \frac{\epsilon_1 S}{p}. \quad (2)$$

In order to design the C band LH metamaterial, Eqs (1) and (2) are first used to obtain an approximate estimate, where the resonances of the SSRR would occur. These estimates deal with the strip-line widths, the gaps, the segment lengths, and the periodicity of the elements. The dimensions of the SSRR structure are finalized using the CST's MWS simulation tools. As shown in Figure 3, the simulation model consisted of a two-port waveguide, formed by a pair of both perfect electric conductor (PEC) and perfect magnetic conductor (PMC) walls. The waveguide is filled with uniform dielectric material with relative permittivity of 2.2, and four SSRRs are centered in the waveguide. The plane wave is transmitted from Port 1 to Port 2 of the waveguide. This model allows the effective simulation of a semi-infinite slab with an infinite periodic array of inclusions illuminated by a normally incident plane wave. All S -parameter values are calculated. The dimensions of the SSRR structure determined are indicated as shown in Figure 4. In addition, the spacing between two PMC boundaries, i.e., the SSRR period along Y direction, is 0.26 mm; the spacing between two PEC boundaries, i.e., the SSRR period along Z direction, is 2.29 mm, and the metal applied to the SSRR is copper.

The MWS predicted magnitude and phase of S -parameters are shown in Figure 5. From Figure 5(a) it can be seen that the magnitude of S_{21} is more than -4 dB, corresponding to a loss less

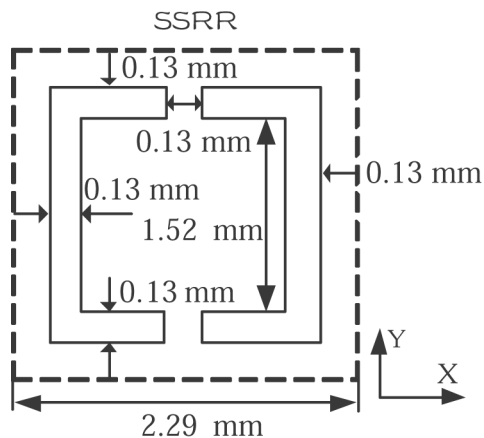
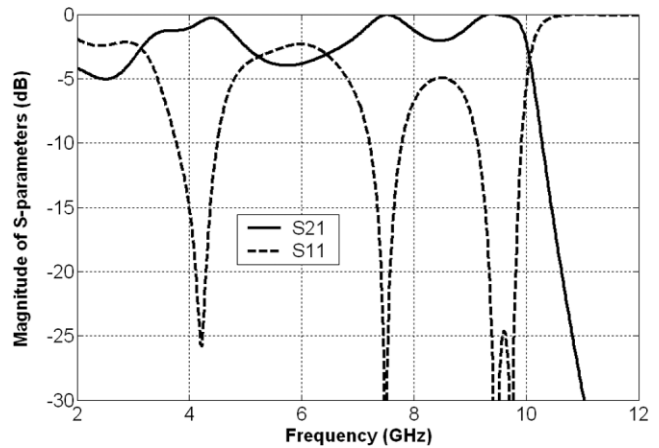
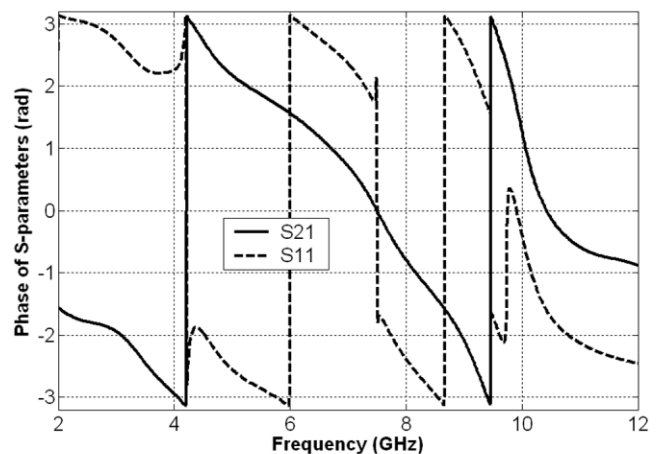


Figure 4 Illustration of dimensions of SSRR



(a)



(b)

Figure 5 (a) Microwave studio predicted magnitude of S -parameters for the LH metamaterial. (b) Microwave studio predicted phase of S -parameters for the LH metamaterial

than 1 dB for every unit cell, in 4.2~7.5 GHz. In addition, there is no obvious abnormality in both the amplitude-frequency curves and the phase-frequency curves of S -parameters, and the frequency band where the LH metamaterial is available cannot be directly seen from such S -parameters. However, the effective permittivity

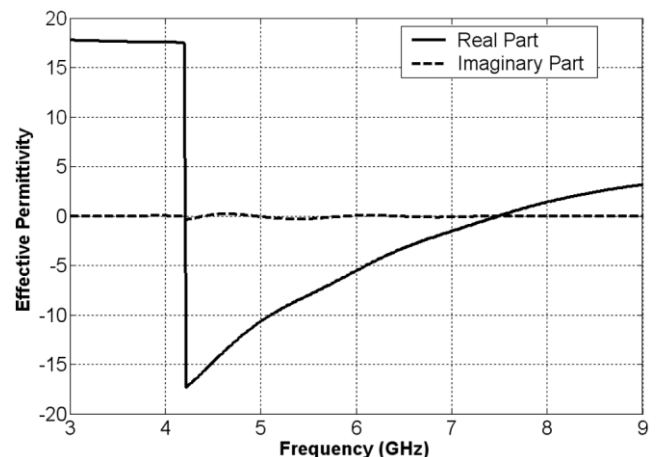


Figure 6 Effective permittivity extracted from the S_{11} and S_{21}

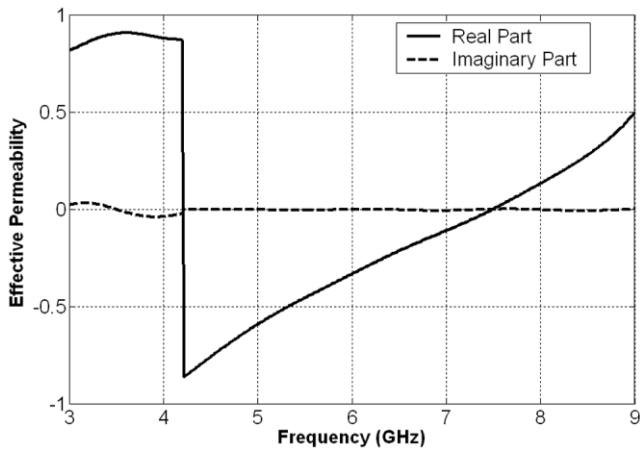


Figure 7 Effective permeability extracted from the S_{11} and S_{21}

and effective permeability of the LH metamaterial slab can be extracted from the S -parameters with NRW approach.

3. VERIFICATION OF DNG PROPERTY

Although it is stated in Ref. 6 that the NRW extraction expressions is unsatisfactory in, the NRW extraction expressions, after testing them on numerous MTM cases, is found to be accurate in most of the frequency regions except, where the values of permittivity and permeability resonances vary quickly between positive and negative values. The real and imaginary parts of effective permittivity are drawn in Figure 6, and the real and imaginary parts of effective permeability are drawn in Figure 7. From Figures 6 and 7, it can be seen that the real parts of effective permittivity and effective permeability are simultaneously negative in 4.2~7.5 GHz, while the imaginary parts approach zero. Other parameters such as phase velocity, wave number, and the index of refraction have also been extracted with the NRW approach, although the data are not shown here. Results show that the velocity, wave number, and the real part of refraction are also negative in 4.2~7.5 GHz.

In addition, to verify the DNG property shown in Figures 6 and 7 an equivalent method is used. First, the four SSRRs are removed in the waveguide, shown in Figure 3, keeping the PMC and the PEC. Second, an ideal uniform LH metamaterial slab with the same relative permittivity, as shown in Figure 6, and the same relative permeability, as shown in Figure 7, is centered in the

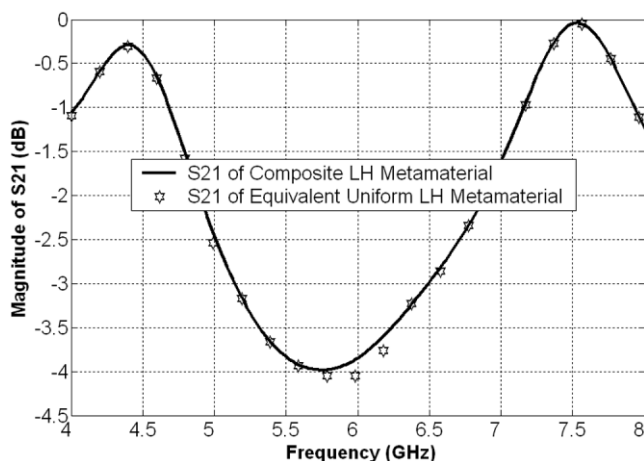


Figure 8 Comparison between magnitudes of S_{21} and S'_{21}

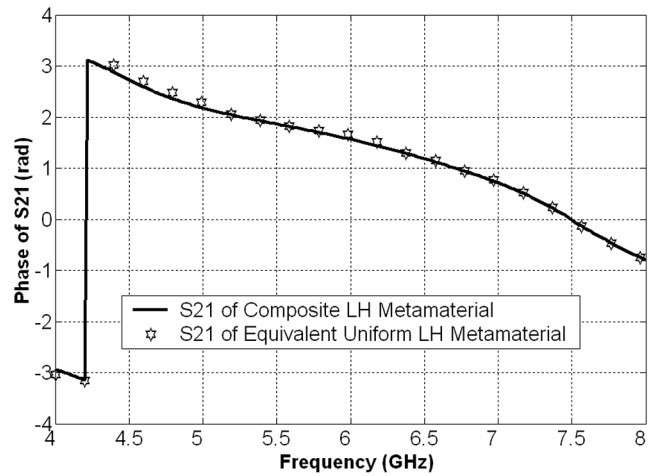


Figure 9 Comparison between phases of S_{21} and S'_{21}

waveguide, and the slab sizes in X , Y , and Z directions are 9.16, 2.29, and 0.254 mm, respectively. Attention is to be paid to the fact that the relative permittivity and the relative permeability can be described by the Drude model in the MWS, when the values are less than one. Third, the input plane wave is launched in uniform medium with relative permittivity of 2.2 toward the slab from each port. S -parameters (S'_{11} and S'_{21}) are calculated and compared with S_{21} and S_{11} . The comparison between magnitudes of S_{21} and S'_{21} is shown in Figure 8, and the comparison between phases of S_{21} and S'_{21} is shown in Figure 9. It can be seen that S_{21} is in a good agreement with S'_{21} for both phases and magnitudes.

4. DISCUSSION

The relative bandwidth of the proposed LH metamaterial can be computed as the ratio of the bandwidth of the left-handed frequency band to its central frequency to compare the bandwidth of the previously reported LH metamaterial structures with the bandwidth of the LH metamaterial constructed from SSRR presented here [8]. The unit cell electrical size at central frequency of the left-handed frequency band compare well with the unit cell size of the previously reported LH metamaterial structures with the unit cell size of the LH metamaterial constructed from SSRR presented here. The results are shown in Table 1, from which it can be seen that the relative bandwidth for the structure proposed in this article appears to be quite wide among the existing publications and its unit cell electrical size appears to be smallest.

Moreover, the central frequency of the LH metamaterial can be tuned by changing the SSRR period along Z direction while the relative bandwidth is fixed. The effective permittivity and effective permeability, when the SSRR period along Z direction, is 2.03 mm and are shown in Figure 10. It can be seen that the real part of effective permittivity and effective permeability are simulta-

TABLE 1 Comparison of the Relative Bandwidths for Different LH Metamaterial Structures

	Structures			
	CLSs/SRRs [6]	Double S [8]	SRR/Rods [7]	SSRR
Relative bandwidth	3.2%	46%	12.2%	56.4%
Unit cell electrical size	0.18	0.12	0.16	0.067

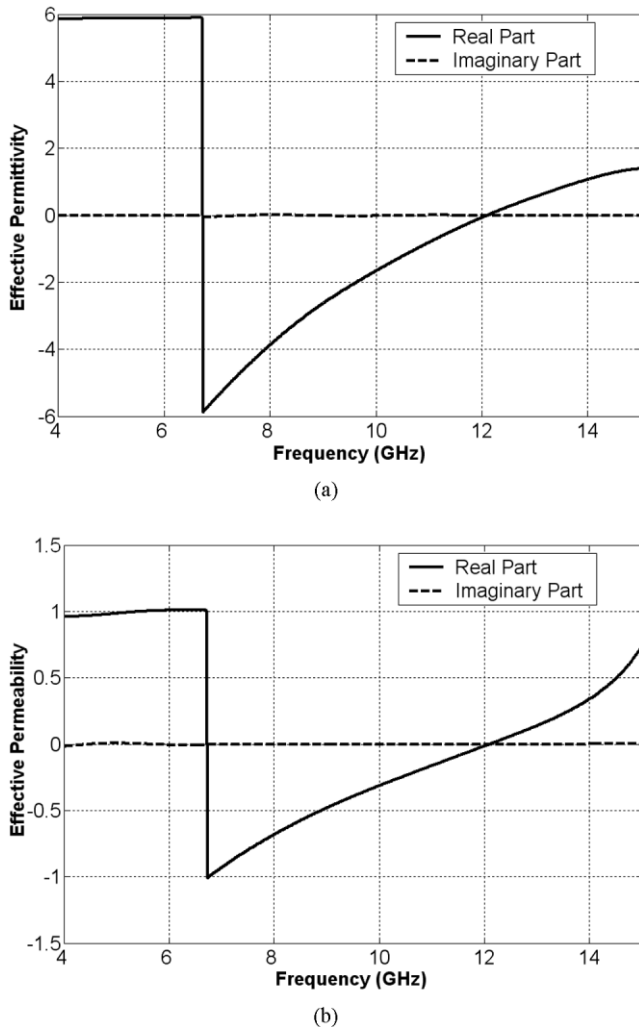


Figure 10 (a) Effective permittivity when the SSRR's period along Z direction is 2.03 mm. (b) Effective permeability when the SSRR's period along Z direction is 2.03 mm

neously negative in 6.8–12 GHz, i.e., the central frequency is shifted to 9.4 GHz.

5. CONCLUSION

The C band LH metamaterial with miniaturized unit cell and broad bandwidth is designed by directly exciting the shunt inductance and series capacitance in the propagation direction of the electromagnetic wave. The relative bandwidth of the LH metamaterial proposed here is 56.4%, and the unit cell electrical size is 0.067. Moreover, the central frequency of the LH metamaterial can be tuned by changing the SSRR period along Z direction while keeping the relative bandwidth. The DNG property is shown by the simultaneous negative effective permittivity and effective permeability extracted from the transmission and reflection data of LH metamaterial slab, and it is confirmed by the equivalent method which is described in detail in this article.

ACKNOWLEDGMENT

This work was supported by the Natural Science Foundation of China under the grant 60571026, and the National Key Laboratory of Electromagnetic Environment under the grant 514860303.

REFERENCES

1. J.B. Pendry, A chiral route to negative refraction, *Science* 306 (2004), 1353–1355.
2. V.G. Veselago, The electrodynamics of substances with simultaneously negative values of ϵ and μ , *Sov Phys Usp* 10 (1968), 509–511.
3. J.B. Pendry, A.J. Holden, D.J. Robbins, and W.J. Stewart, Low frequency plasmons in thin-wire structures, *J Phys: Condens Matter* 10 (1998), 4785–4809.
4. J.B. Pendry, A.J. Holden, D.J. Robbins, and W.J. Stewart, Magnetism from conductors and enhanced nonlinear phenomena, *IEEE Trans Microwave Theory Tech* 47 (1999), 2075–2084.
5. D.R. Smith and N. Kroll, Negative refractive index in left-handed materials, *Phys Rev Lett* 85 (2000), 2933–2936.
6. R.W. Ziolkowski, Design, fabrication, and testing of double negative metamaterials, *IEEE Trans Antennas Propag* 51 (2003), 1516–1529.
7. D.R. Smith, P. Rye, D.C. Vier, A.F. Starr, J.J. Mock, and T. Perram, Design and measurement of anisotropic metamaterials that exhibit negative refraction, *IEICE Trans Electron E87-C* (2004), 359.
8. H. Chen, L. Ran, J. Huangfu, X. Zhang, K. Chen, T.M. Grzegorzcyk, and J.A. Kong, Negative refraction of a combined double s-shaped metamaterial, *Appl Phys Lett* 86 (2005), 1–3.
9. C. Caloz and T. Itoh, Application of the transmission line theory of left-handed (LH) materials to the realization of a microstrip LH line, In: *AP-S International Symposium (Digest), IEEE Antennas and Propagation Society, 2002*, pp. 412–415.

© 2006 Wiley Periodicals, Inc.

HIGH-POWER NARROW LINE WIDTH TUNABLE CLADDING PUMPED ER:YB CO-DOPED FIBER LASER

Shu-min Zhang,^{1,2} Fu-yun Lu,² and Jian Wang²

¹ Department of Physics
Hebei Normal University
Shijiazhuang, 050016, China

² Institute of Physics
Nankai University
Tianjin, 300071, China

Received 11 February 2006

ABSTRACT: A narrow line width, tunable, and highly efficient fiber laser based on Er^{3+}/Yb^{3+} co-doped double-clad fiber with the maximum output power of 438 mW and a slope efficiency of $\sim 16\%$ has been demonstrated. By using a fiber Bragg grating (FBG) as a narrow band reflector, 3-dB line width of the output laser could be as narrow as 0.04 nm over the whole tuning range, and by compressing or stretching the FBG, wavelength tunable range of 4.0 nm was realized. In the experiment, we also found that there existed an optimum splitting ratio of the output coupler, at which the maximum output power could reach ~ 647 mW. © 2006 Wiley Periodicals, Inc. *Microwave Opt Technol Lett* 48: 1736–1739, 2006; Published online in Wiley InterScience (www.interscience.wiley.com). DOI 10.1002/mop.21762

Key words: high-power; narrow-line width; tunable fiber ring laser; cladding-pump

1. INTRODUCTION

In recent years there has been growing interest in fiber lasers. Their main advantages are a simple setup with a small number of adjustable components and the compatibility of optical components used in telecommunication systems. Moreover, because of their broad emission spectrum and the novel fiber designs such as double-clad fibers, these lasers are also useful for the generation of wavelength tunable narrow line width high power laser. Auerbach